

Anatomical correlates of the functional organization in the human occipitotemporal cortex

Mina Kim^a, Mathieu Ducros^b, Thomas Carlson^{c,d}, Itamar Ronen^f, Sheng He^e,
Kamil Ugurbil^a, Dae-Shik Kim^{f,*}

^aCenter for Magnetic Resonance Research, University of Minnesota, Minneapolis, MN, USA

^bLaboratoire de Neurophysiologie et Nouvelles Microscopies, ESPCI-INSERM EPI 00-02 Paris, France

^cDepartment of Psychology, Vision Sciences Laboratory, Harvard University, Cambridge, MA 02138, USA

^dDepartment of Psychonomics, Utrecht University, Utrecht, The Netherlands

^eDepartment of Psychology, University of Minnesota, Minneapolis, MN 55455, USA

^fCenter for Biomedical Imaging (CBI), Department of Anatomy and Neurobiology, Boston University school of Medicine, Boston, MA 02118, USA

Received 30 June 2005; accepted 9 December 2005

Abstract

The connectivity between functionally distinct areas in the human brain is unknown because of the limitations posed by current postmortem anatomical labeling techniques. Diffusion tensor imaging (DTI) has previously been used to define large white matter tracts based on well-known anatomical landmarks in the living human brain. In the present study, we used DTI coupled with functional magnetic resonance imaging (fMRI) to assess neuronal connections between human striate and functionally defined extrastriate ventral cortical areas. Functional areas were identified with conventional fMRI mapping procedures and then used as seeding points in a DTI analysis to ascertain connectivity patterns between cortical areas, thus yielding the pattern of connections between human occipitotemporal visual areas in vivo.

© 2006 Elsevier Inc. All rights reserved.

Keywords: fMRI; DTI; Fiber tracking; Human ventral cortex

1. Introduction

A central feature of the mammalian visual system is the presence of multiple visual areas. The number of areas range from 10 to 15 for cats [1] and 20 to 30 for macaques [2]. In humans, the exact number of visual areas is unknown [3], but there is reason to believe that it exceeds the number of macaque visual areas. Like other primates, human visual areas are clustered along two “streams” diverging from the occipital pole: the ventral “what or perception” stream and the dorsal “where or action” stream [4,5]. While the areas in the dorsal stream tend to be tuned for visual stimuli and tasks related to stimulus location and/or action, the ventral stream consists of a web of areas that are selectively tuned for object recognition processes. For example, lateral

occipital cortex (LOC), a region extending anteriorly into the temporal cortex, responds more strongly to objects (e.g., polygonal figures, chairs, and gloves) than to scrambled images [6,7]. More anterior to LOC, the selectivity for object categories is extended even further. Here, the fusiform face area (FFA) [8] responds greatest to faces and facial stimuli (e.g., front-view photographs of faces and line drawings of faces, etc.) in a way comparable to the receptive field properties of face-selective neurons in primate inferotemporal cortex (IT) [9,10]. Further down the temporal cortex, in the so-called parahippocampal place area (PPA) [11], maximum functional response can be obtained using scenic- or place-type stimuli. The way in which object category-specificity emerges along the human ventral stream given the fundamentally object category indifferent receptive field properties in the early stages of the visual pathway (retina, lateral geniculate nucleus, V1/V2) remains elusive.

* Corresponding author. Tel.: +1 617 414 2361; fax: +1 617 414 2362.
E-mail address: dskim@bu.edu (D.-S. Kim).

In nonhuman primates, object category-selective areas in the ventral stream are interlinked with striate cortex through a pattern of highly characteristic connections. This precise arrangement of inter-areal connections — together with intra-area local and long-range horizontal connections — is thought to give rise to the complex receptive field properties of object category-selective neurons. In humans, the pattern of connections between functionally defined visual areas is unknown because conventional neuroanatomical approaches, such as degeneration [12], postmortem [13], and transneuronal tracers [14], are not possible due to their invasive nature.

In the present study, we used diffusion tensor magnetic resonance imaging (DT-MRI) in combination with high-resolution functional magnetic resonance imaging (fMRI) to label the pattern of connections between object category-selective areas in the human occipitoventral cortex in a noninvasive manner. Several neuroimaging studies have successfully combined functional with structural measures in the human visual system [15,16]. Werring et al. [15] overlaid fMRI visual activation maps on to corresponding fractional anisotropy (FA) maps, and Toosy et al. [16] demonstrated optic radiations using the probabilistic index of connectivity [17].

Diffusion tensor imaging (DTI) is a technique in which the presence and orientation of axonal fibers are reconstructed through careful measurement of intravoxel water diffusion [18]. In a medium restricted by physical structures, such as bundles of axonal fibers, water diffusion is anisotropic, with the principal direction of anisotropy parallel to the direction of the fibers. Recently, a combination of DTI and three-dimensional (3D) fiber reconstruction algorithms has been used to generate robust images of axonal connectivity in humans [19], rodents [20] and cats [21]. Responses to visual stimulation were recorded with echo-planar fMRI and analyzed with conventional methods. The resulting fMRI data sets were coregistered with DTI images collected separately from each subject. The coregistered fMRI/DTI data were used to simultaneously and noninvasively assess the relationship between functional activity and neuronal connectivity within the human ventral stream.

2. Experimental procedures

2.1. Subjects

Four healthy volunteers (one female, three males, ages 23–30 years) were enrolled in the study after giving written and informed consent. All subjects were given detailed instructions of the experiment both inside and outside the scanner before the actual scan. All experimental procedures were approved by the University of Minnesota Institutional Review Board and are in compliance with guidelines published by the National Institutes of Health (USA).

2.2. Stimuli

Visual stimuli were generated on a G4 Macintosh Computer, using custom-written MATLAB (The Mathworks, Natick, MA) software utilizing functions provided by PsychToolbox [22]. Stimuli were presented binocularly with a video projector on a rear projection screen. Retinotopic visual areas were mapped with conventional checkerboard stimuli consisting of four triangular wedges and four segmented expanding rings. Localizer stimuli known to activate respective areas within the human ventral stream were used to identify the FFA (conventional/scrambled faces) [23], PPA (buildings and scenes), and LOC (set of complex objects) (Fig. 1B). Within each all-novel epoch (24 s each), subjects saw four categories of pictures that each contained 30 different photographs. Within multiple-repeat epochs (four repetitions), subjects saw different photographs from the same category. A separate localizer (moving dots) was used to identify the human mediotemporal area (hMT+, motion) as part of the human dorsal stream. This scan consisted of moving dots contrasted with stationary dots as a control.

2.3. MRI acquisition

MR studies were performed with a conventional 3-T clinical scanner (Siemens Trio, Germany). A circularly polarized head coil was used to transmit/receive (TR) the MR signal. Each subject was presented with three to four different types of stimuli, each optimized to elicit BOLD activation in the areas of interest (retinotopy, motion stimuli, and ventral stream stimuli).

Gradient-echo, echo-planar imaging (EPI) was used with typical imaging parameters (TR, 3 s; TE, 40 ms; 128×128

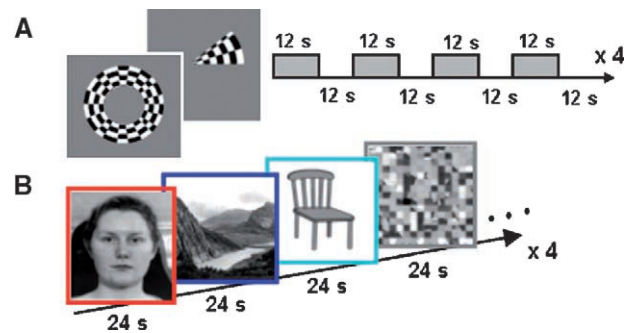


Fig. 1. Experimental design. Checkerboard stimuli were presented for retinotopic delineation (panel A). Each stimulus consisted of four triangular wedges for upper/lower and left/right visual field, and four segmented expanding rings. Each segment was presented for 12 s followed by a blank period of 12 s, and repeated four times. Panel B shows example localizer stimuli used to activate ventral visual areas. Stimuli included images of buildings and scenes (for PPA), pictures of human faces (for FFA), a set of complex objects (for LOC), and scrambled images (control). Each category of pictures contained 30 different photographs that were presented for 24 s followed by a different category for the same duration. Within multiple-repeat epochs (four repetitions), subjects saw different photographs in the same category. For the hMT+ stimulus (motion) (not shown here), the moving dots were contrasted with stationary dots as a control.

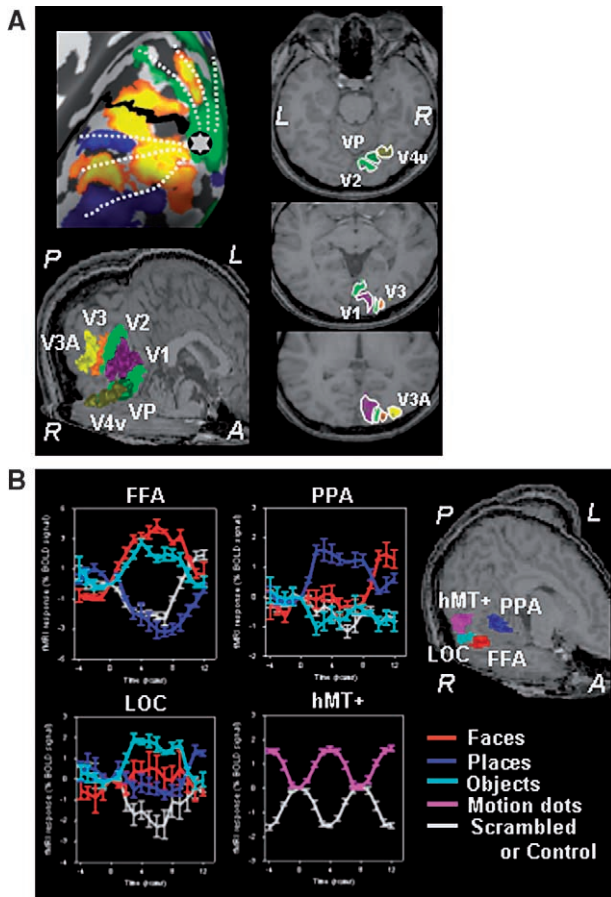


Fig. 2. Volume-rendered representation of visual areas and the experimental protocol. Panel A shows the 3D volume-rendered retinotopic layout in one of the subjects (S1) from checkerboard stimuli (A). The right figure of panel A displays the positions of the volume-rendered retinotopic visual areas (the left bottom row) in a series of in-plane images. The right figure in panel B shows the 3D volume-rendered ventral areas and motion area obtained by the localizer stimuli in subject S1 from the series of localizer stimuli used to activate the ventral visual areas. The left graphs show the time courses depicting the tuning behavior of the respective areas. Error bars indicate S.E.M. A, anterior; P, posterior; L, left; R, right.

in a FOV of 256×256 mm²; native resolution, 2 mm isovoxel). Thirty 2-mm-thick axial slices covered the occipital lobes as well as the ventrotemporal cortex. Each fMRI scan lasted about 6.5 min.

In the same session, DTI was performed with spin-echo EPI and conventional parameters (TR, 11.5 s; TE, 111 ms; 128×128 in a FOV of 256×256 mm²; native resolution, 2 mm isovoxel). DWI signals were averaged (number of excitation=3) to increase SNR. Total acquisition time was 7 min and 40 s. We were able to shorten the acquisition time significantly through the use of a 3-T magnet. Twelve directions of gradient-encoded diffusion-weighted images were used with $b=1000$ s/mm². One reference image with no diffusion weighting was also acquired.

T₁-weighted high resolution (1 mm³ isovoxel) anatomical images were obtained from each subject to allow accurate cortical segmentation and inflation.

2.4. Data analysis

Functional imaging scans were used to localize areas hMT+, LOC, FFA, PPA, and retinotopic areas (V1, V2, V3, V3A, VP and V4v) in each subject. fMRI activations were visualized on 3D-inflated (surface-based) or flattened cortical maps, and then exported as thirty two-dimensional maps taken along the z direction using BrainVoyager (Brain Innovation, Maastricht, The Netherlands). These maps were coregistered with 3D DTI data from the same subject using custom-written DTI reconstruction software.

Diffusion tensors, FA, and fiber tracts were calculated using custom-written MATLAB (The Mathworks) software. Standard methods for FA exclusion and tracking algorithms were used [24], that is, minimum FA of 0.2 and 60° of maximum angle. Since fMRI activation is limited to the gray/white matter border, we chose to include at least one more voxel (beyond the gray/white matter boundary) into our seeding region of interest (ROI) when the fMRI ROI included only gray matter. To investigate the connectivity pattern, an automated DTI fiber tracking procedure was performed. DTI fiber trajectories were computed systematically between pairs of functionally defined ROIs (i.e., V1 and PPA, V2 and FFA, etc.) with an automated fiber-tracking algorithm [24]. These fiber trajectories were then superimposed on 3D anatomical images for visualization.

2.5. Fiber reconstruction reliability

Due to the noise inherent in all MR images, there is uncertainty associated with every estimate of fiber orientation. In tractography, accumulated uncertainties in fiber orientation could potentially lead to erroneous fiber reconstructions. To quantify the uncertainty in the connectivity patterns presented in this study, we measured an uncertainty angle (UA) at every point along the fiber using the “bootstrapping” method described by Jones [25]. Bootstrapping allows us to assess whether the obtained fiber reconstruction results were influenced by stochastic effects. To this end, we created 100 pseudoreplicate data sets by adding random noise to the original diffusion-weighted data. The noise level was set to 0.1% of the maximum signal, which corresponds to the original image’s SNR. For each bootstrap sample, we computed the eigenvector of the dyadic tensor [26].

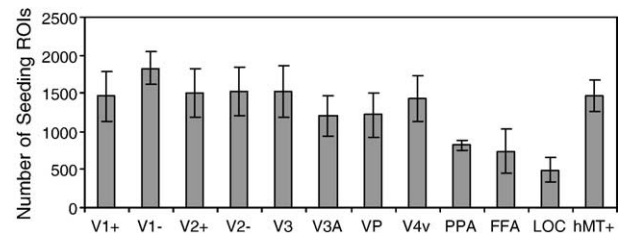


Fig. 3. Mean number and S.E. of seeding ROIs across four subjects. The graph shows the number of seeds that were evaluated for early visual areas and higher visual areas.

For the purpose of inferring the overall uncertainty in a single data set, 100 resamples are generated, yielding a voxelwise distribution of DTI-derived values (e.g., FA) from which the 95% confidence interval (CI) is extracted [27]. UA is equal to the uncertainty in the estimate of the orientation of the principle eigenvector for a given CI. A UA close to 0° indicates a high reliability of the measured eigenvectors, whereas UA close to 90° indicates eigenvectors that are not reliable. In the tracking algorithm we used here [24], the local fiber orientation is parallel to the eigenvector. Therefore, the average UA of all points along a bundle of fibers provides a quantitative measure of the reliability of the connectivity between two areas. By calculating the UAs of a fiber bundle, we can quantify the precision of the estimated connectivity patterns and fiber orientations, rather than accuracy.

3. Results

Here we describe primary and visual association areas delineated by a variety of previously validated functional paradigms: V1/V2 (checkerboard), hMT+ (motion field), LOC (complex objects), FFA (conventional/scrambled faces) and PPA (buildings and scenes).

Our first goal was to identify functional clusters in retinotopic and ventral/dorsal areas for use as seeding ROIs. These functionally based ROIs define a new type of cortical parcellation, and thus our connectivity results may differ from classical tractography work.

Four human subjects were scanned using fMRI, DTI and anatomical sequences. In our first procedure, conventional checkerboard stimuli in a block design were presented to delineate retinotopic areas (Fig. 1A). Then, a series of localizer stimuli including buildings and scenes (for PPA), conventional faces (for FFA), a set of complex objects (for LOC) and scrambled textures (for control) were used to activate ventral visual areas (Fig. 1B). For hMT+ (motion field), moving dots were shown separately and contrasted with stationary dots as a control. fMRI data were collected in separate sessions and analyzed with using the general linear model with BrainVoyager software. DTI scans were performed immediately following fMRI scans (without moving the subject) and analyzed with conventional fiber reconstruction procedures. Finally, T₁-weighted high-resolution (1 mm³ isovoxel) anatomical images were obtained for each subject to allow accurate cortical segmentation and inflation.

Panels in Fig. 1 display examples of stimuli used for initial localization of visual areas along the human occipitoventral stream. Expanding rings and rotating wedges were used to delineate the retinotopic borders between V1, V2, V3, V3A, VP and V4v (see details in Figs. 1A and 2A). Localizer stimuli were used to selectively activate the areas of hMT+, LOC, FFA, and PPA (see Figs. 1B and 2B).

Fig. 2 shows the surface tangents of the individual areas which were volume rendered to yield 3D reconstruction of

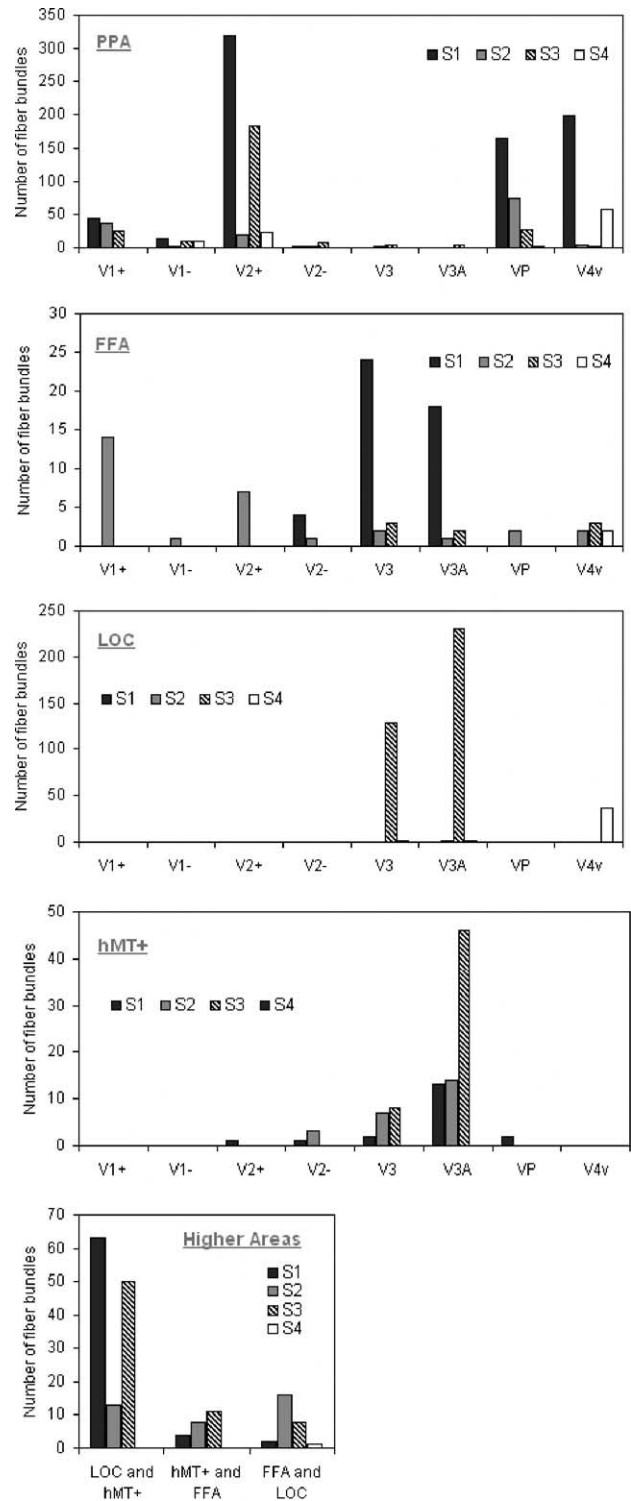


Fig. 4. Observed connections. Bar graphs represent the number of fibers between retinotopic and ventral/dorsal areas (PPA, FFA, LOC and hMT+), and fibers connecting ventral and dorsal ROIs (higher areas) for each of the four subjects (S1, S2, S3 and S4). The figure shows connections among hMT+, FFA and LOC forming a loop between these areas, but not with PPA, observed in at least three subjects.

the respective visual areas for one of the four subjects (S1). Panel 2A displays the positions of the volume-rendered retinotopic visual areas in a series of in-plane images. For “higher,” nonretinotopic areas, standard “localizer” stimuli — such as depicted in panel 2B — were used to selectively activate the areas PPA, FFA, LOC and hMT+. All fMRI clusters were chosen by strong activation [$P < .0001$ (uncorrected)]. For the present study, we did not distinguish between the retinotopic (MT) and the nonretinotopic (MST) [28] subdivisions of hMT+. Normalized Talairach coordinates of the investigated areas were found to be in good agreement with previous published results; hMT+: 46, -58, 4; LOC: 46, -63, 8; FFA: 36, -48, -16; and PPA: 28, -39,

–6. Following the initial localization, voxels from retinotopic and nonretinotopic functional areas were used as “seeding” points for DTI-based fiber reconstructions.

Fig. 3 shows the number of seed ROIs that were evaluated for each purported connection in each experiment. The number of seeding ROIs in early visual areas was in the range of 1000–2000 on average, and ventral seeding ROIs (PPA, FFA and LOC) were in the range of 500 to 1000 while seeds for motion area (hMT+) were around 1500.

Since the validity of the reported results depends heavily on the choice of ROI seeds and the tractography technique employed, it is important to perform control tract tracing experiments between all the activated areas studied. The

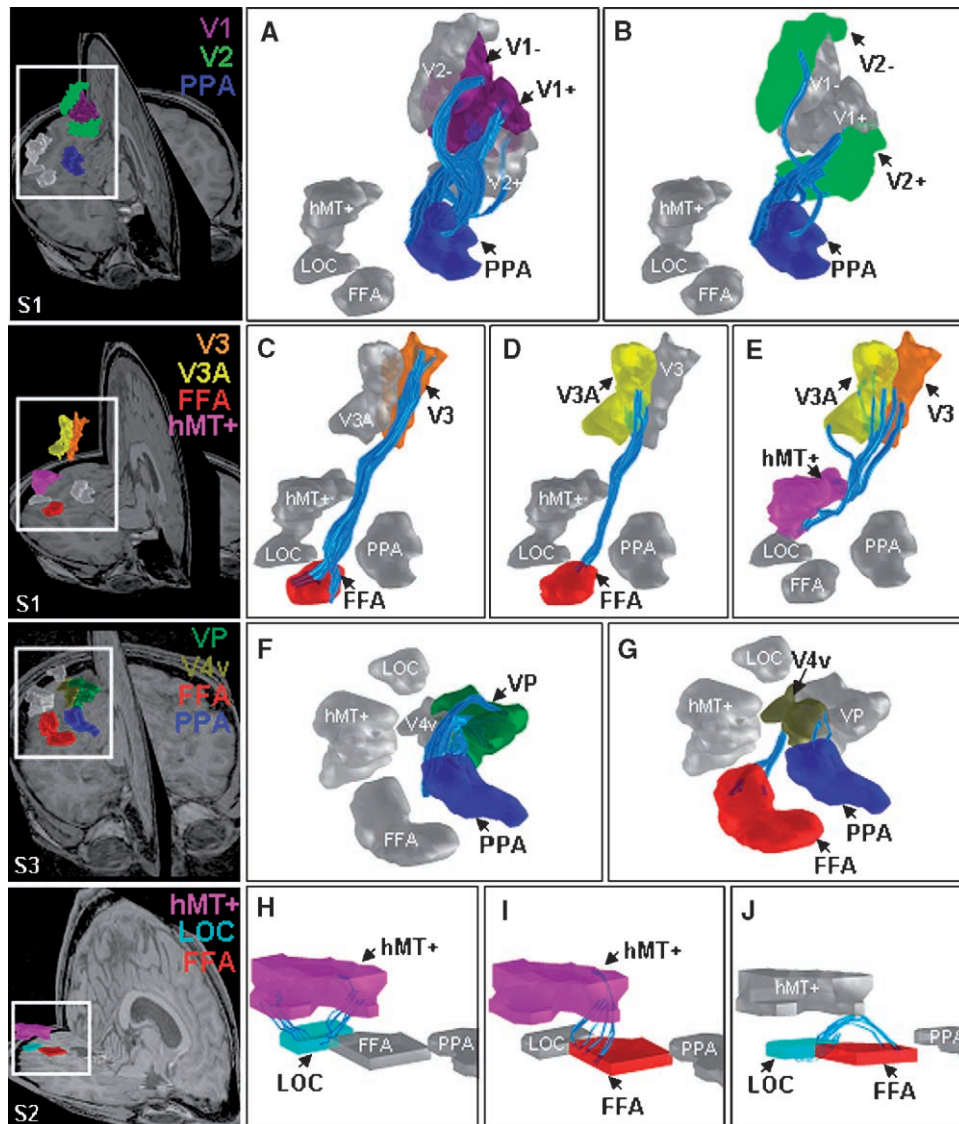


Fig. 5. Visualization of reconstructed fiber connections between each set of ROIs. The left-most figures are 3D anatomical images containing the ROIs from which connections have been observed. Panels A and B show connections between V1/V2 and PPA (obtained from all four subjects) in subject S1 (color-labeled as purple for V1, green for V2). Panels C–E show connections between V3/V3A and FFA, and between V3/V3A and hMT+ (obtained from three subjects) in subject S1 (color-labeled as orange for V3, yellow for V3A). Panels F and G show connections between VP/V4v and PPA (obtained from four subjects), and between V4v and FFA (obtained from three subjects) in subject S3 (color-labeled as dark green for VP, olive green for V4v). Panels H–J show loop-like connections between hMT+, LOC and FFA (obtained from greater than three subjects). Color-labeled as blue for PPA, red for FFA, light blue for LOC and pink for hMT+.

appear to be included within this ventrotemporal loop. PPA was found to connect almost exclusively with more retinotopic areas, such as V1/V2, VP and V4v. These fiber bundles were observed in three or four subjects. Each panel shows multiple seeds in one subject. In panel G, single-seed foci projected to both FFA and PPA.

4. Discussion

The use of activation clusters as tractography seeds is a unique methodology for identifying functionally important areas and their connectivity without relying on anatomical landmarks or to justify the delineation of functional areas.

In the present study, the structure–function relationships between areas of the human occipitoventral stream were assessed using the noninvasive magnetic resonance techniques of fMRI and DT-MRI. While recent data suggest an approximate linearity between fMRI and neuronal activities [29,30], the veracity of DTI-based fiber reconstruction remains inconclusive. For example, the relative contribution of fiber density and myelination on the anisotropy index is not completely understood. Thus, the degree to which DTI results correspond to actual axonal fiber bundles is not clear. Moreover, DTI provides information on connectivity, but fails to yield information on the directionality of the fibers. However, several lines of evidences suggest the parsimonious veracity of DTI-based fiber reconstructions. All major fiber bundles investigated in humans so far (corpus callosum [31], internal capsule [24], corticospinal tract [32]) are in agreement with the fiber orientation/geometry obtained using more traditional tracing techniques. Furthermore, coinjection of the MRI-sensitive *in vivo* fiber tract tracer [33] manganese ion Mn^{2+} suggests that DTI-based reconstructions and Mn^{2+} -labeled fibers are closely coregistered [34]. Taken together, we are aware of the current lack of direct evidence supporting the validity of DTI-based fiber reconstruction; however, we believe there is sufficient circumstantial evidence to support its use, especially if the data are interpreted in conjunction with homologous neurotracing data from nonhuman primates. For example, in rhesus macaques, it has been found that the ventral visual processing stream has strong connections between occipital and temporal lobe association cortices [35]. Consistent with these classical tractography observations, our DTI results suggest that V1 and V2 are crucial to processing places and scenes (PPA) and confirm that PPA in humans is specialized for processing place stimuli. These areas were found to have the highest connectivity among the small cluster of areas in the ventral stream.

The results of our study also suggest that the human occipitoventral stream is governed by a distinct pattern of inter-areal connectivities.

Fig. 6 summarizes our results. Observed connections are classified into two groups: “certain,” and “less certain” depending on their occurrence in all (certain), or three of four (less certain) of the studied subjects. While FFA and

LOC share many common receptive field properties, PPA seems to take a rather odd position in terms of its pattern of connectivity. Moreover, areas hMT+, LOC and FFA are tightly interconnected, forming a loop for processing visual information. The principal connections to/from this ventral loop are provided by areas V3 and V3A, while the influence of the primary visual areas V1 and V2 to/from this processing loop is limited. The observed connections between V3/V3A/V4v and FFA (Fig. 4C, D and G) seem to be consistent with the hierarchical pattern of visual areas observed in macaques [36]: similar to macaque IT cortex (area TE), human FFA does not receive direct projections from V1/V2. While macaque TE receives direct input only from V4v [2], our data show direct connections between human FFA and V4v/V3/V3A. Due to the ambiguous directionality, we are unable to determine which connections are feed forward or backward. In macaque, area MT receives direct connections from V1/V2/V3 [37], and our results present that human MT+ also receives direct connection from V3. However, we were unable to confirm the homologous direct connections between V1/V2 and hMT+ as the UA values along this tract were too large to rule out the possibility of erroneous sharply turned fibers during the fiber tractography computation.

Surprisingly, PPA was not found to be part of the ventral loop. PPA might form a separate, more “linear” processing pathway with more direct links to areas V1/V2, VP and V4v (see Figs. 4–6). V1 projects largely to PPA, but projections from V1+ are dominated by interhemispheric fibers passing through the corpus callosum. This may explain why there is a large asymmetry from V1+ and V1– (and V2+ and V2–) to PPA. Understanding this peculiar placement of PPA is difficult because, thus far, no macaque homologue for PPA has been firmly established. The functional and developmental significance of this lack of interaction with other categorical areas (such as FFA and LOC) remains to be studied. It will be fascinating to investigate this contrast in structure/function relationships between FFA/LOC and PPA.

Although our major findings are consistent with well-established connectivity patterns such as direct connections between PPA and primary visual areas V1/V2, there is considerable between-subject variability in the quantity and pattern of fibers between other ROIs. Since each brain is slightly different in shape and size, it is not recommended to normalize white matter structures across subjects. Averaging DTI data sets across subjects can introduce errors into the fiber reconstruction. In our study, each complete data set from each subject is regarded as independent from each other. Therefore, it is necessary to compare the pattern of connections between subjects rather than the number of fibers. However, the variability in fiber existence can arise from a number of sources, such as noise, partial voluming and the tracking algorithm. To improve the analysis, it may help to examine more subjects, acquire DTI acquisitions with higher spatial resolution and compare results from different tracking algorithms.

Finally, despite the consistency of the reported major connectivity patterns, it is still unclear whether the ROIs are functionally connected since ROIs were acquired from separate functional paradigms, then pooled together to assess connectivity from the DT-MRI data. Therefore, the results reported here only suggest the existence of anatomical connections between ROIs. One method of validation for the loop connectivity would be to devise a functional paradigm that activates hMT+, LOC and FFA simultaneously. Tests of topographic relationships could be performed with more effective connectivity experiments (causality in order to determine if those areas are functionally and/or anatomically heterogeneous). Such a paradigm may provide a functional validation of the loop and tractography seeds in the same data set.

Acknowledgments

The authors thank Dr. J. Thompson for editorial help. This work was supported by NIH (RR08079, NS44825, EB00331), the Keck Foundation, and the Human Frontiers Science Program.

References

- [1] Payne BR, Peters A. The cat primary visual cortex. San Diego: Academic Press; 2002.
- [2] Felleman DJ, Van Essen DC. Distributed hierarchical processing in the primate cerebral cortex. *Cereb Cortex* 1991;1(1):1–47.
- [3] Tootell RB, Dale AM, Sereno MI, Malach R. New images from human visual cortex. *Trends Neurosci* 1996;19(11):481–9.
- [4] Ungerleider LG, Haxby JV. ‘What’ and ‘where’ in the human brain. *Curr Opin Neurobiol* 1994;4(2):157–65.
- [5] Goodale MA, Milner AD. Separate visual pathways for perception and action. *Trends Neurosci*; 1992. p. 20–5.
- [6] Malach R, Levy I, Hasson U. The topography of high-order human object areas. *Trends Cogn Sci* 2002;6(4):176–84.
- [7] Grill-Spector K. The neural basis of object perception. *Curr Opin Neurobiol* 2003;13(2):159–66.
- [8] Kanwisher N, McDermott J, Chun MM. The fusiform face area: a module in human extrastriate cortex specialized for face perception. *J Neurosci* 1997;17(11):4302–11.
- [9] Tanaka K, Saito H, Fukada Y, Moriya M. Coding visual images of objects in the inferotemporal cortex of the macaque monkey. *J Neurophysiol* 1991;66(1):170–89.
- [10] Desimone R, Albright TD, Gross CG, Bruce C. Stimulus-selective properties of inferior temporal neurons in the macaque. *J Neurosci* 1984;4(8):2051–62.
- [11] Epstein R, Kanwisher N. A cortical representation of the local visual environment. *Nature* 1998;392(6676):598–601.
- [12] Whitlock DG, Nauta WJH. Subcortical projections from temporal neocortex in *Macaca mulatta*. *J Comp Neurol* 1956;106:183–212.
- [13] Galuske RA, Schlote W, Bratzke H, Singer W. Interhemispheric asymmetries of the modular structure in human temporal cortex. *Science* 2000;289(5486):1946–9.
- [14] Katz LC, Iarovici DM. Green fluorescent latex microspheres: a new retrograde tracer. *Neuroscience* 1990;34(2):511–20.
- [15] Werring DJ, Clark CA, Parker GJ, Miller DH, Thompson AJ, Barker GJ. A direct demonstration of both structure and function in the visual system: combining diffusion tensor imaging with functional magnetic resonance imaging. *Neuroimage* 1999;9(3):352–61.
- [16] Toosy AT, Ciccarelli O, Parker GJ, Wheeler-Kingshott CA, Miller DH, Thompson AJ. Characterizing function–structure relationships in the human visual system with functional MRI and diffusion tensor imaging. *Neuroimage* 2004;21(4):1452–63.
- [17] Parker GJ, Haroon HA, Wheeler-Kingshott CA. A framework for a streamline-based probabilistic index of connectivity (PICO) using a structural interpretation of MRI diffusion measurements. *J Magn Reson Imaging* 2003;18(2):242–54.
- [18] Basser PJ, Mattiello J, LeBihan D. MR diffusion tensor spectroscopy and imaging. *Biophys J* 1994;66(1):259–67.
- [19] Conturo TE, Lori NF, Cull TS, Akbudak E, Snyder AZ, Shimony JS, et al. Tracking neuronal fiber pathways in the living human brain. *Proc Natl Acad Sci U S A* 1999;96(18):10422–7.
- [20] Mori S, Crain BJ, Chacko VP, van Zijl PC. Three-dimensional tracking of axonal projections in the brain by magnetic resonance imaging. *Ann Neurol* 1999;45(2):265–9.
- [21] Kim DS, Kim M, Ronen I, Formisano E, Kim KH, Ugurbil K, et al. In vivo mapping of functional domains and axonal connectivity in cat visual cortex using magnetic resonance imaging. *Magn Reson Imaging* 2003;21(10):1131–40.
- [22] Brainard DH. The psychophysics toolbox. *Spat Vis* 1997;10(4):433–6.
- [23] Blanz V, Vetter T. A morphable model for synthesis of 3D faces. In *Computer Graphics Proceedings SIGGRAPH*. Los Angeles; 1999.
- [24] Basser PJ, Pajevic S, Pierpaoli C, Duda J, Aldroubi A. In vivo fiber tractography using DT-MRI data. *Magn Reson Med* 2000;44(4):625–32.
- [25] Jones DK. Determining and visualizing uncertainty in estimates of fiber orientation from diffusion tensor MRI. *Magn Reson Med* 2003;49(1):7–12.
- [26] Basser PJ, Pajevic S. Statistical artifacts in diffusion tensor MRI (DT-MRI) caused by background noise. *Magn Reson Med* 2000;44(1):41–50.
- [27] Heim S, Hahn K, Samann PG, Fahrmeir L, Auer DP. Assessing DTI data quality using bootstrap analysis. *Magn Reson Med* 2004;52(3):582–9.
- [28] Huk AC, Dougherty RF, Heeger DJ. Retinotopy and functional subdivision of human areas MT and MST. *J Neurosci* 2002;22(16):7195–205.
- [29] Ugurbil K, Toth L, Kim DS. How accurate is magnetic resonance imaging of brain function? *Trends Neurosci* 2003;26(2):108–14.
- [30] Logothetis NK, Pauls J, Augath M, Trinath T, Oeltermann A. Neurophysiological investigation of the basis of the fMRI signal. *Nature* 2001;412(6843):150–7.
- [31] Xu D, Mori S, Solaiyappan M, van Zijl PC, Davatzikos C. A framework for callosal fiber distribution analysis. *Neuroimage* 2002;17(3):1131–43.
- [32] Stieltjes B, Kaufmann WE, van Zijl PC, Fredericksen K, Pearlson GD, Solaiyappan M, et al. Diffusion tensor imaging and axonal tracking in the human brainstem. *Neuroimage* 2001;14(3):723–35.
- [33] Pautler RG, Silva AC, Koretsky AP. In vivo neuronal tract tracing using manganese-enhanced magnetic resonance imaging. *Magn Reson Med* 1998;40(5):740–8.
- [34] Lin CP, Tseng WY, Cheng HC, Chen JH. Validation of diffusion tensor magnetic resonance axonal fiber imaging with registered manganese-enhanced optic tracts. *Neuroimage* 2001;14(5):1035–47.
- [35] Rockland KS, Pandya DN. Cortical connections of the occipital lobe in the rhesus monkey: interconnections between areas 17, 18, 19 and the superior temporal sulcus. *Brain Res* 1981;212(2):249–70.
- [36] Van Essen DC, Anderson CH, Felleman DJ. Information processing in the primate visual system: an integrated systems perspective. *Science* 1992;255(5043):419–23.
- [37] Maunsell JH, van Essen DC. The connections of the middle temporal visual area (MT) and their relationship to a cortical hierarchy in the macaque monkey. *J Neurosci* 1983;3(12):2563–86.